Appl Microbiol Biotechnol (2011) 91:1677–1684
DOI 10.1007/s00253-011-3509-7

BIOENERGY AND BIOFUELS

Kinetics of CO conversion into H_2 by *Carboxydothermus hydrogenoformans*

Ya Zhao · Ruxandra Cimpoia · Zhijun Liu · Serge R. Guiot

Received: 13 June 2011 / Revised: 14 July 2011 / Accepted: 20 July 2011 / Published online: 7 August 2011

Abstract The objective of this study was to improve the biological water–gas shift reaction for producing hydrogen (H_2) by conversion of carbon monoxide (CO) using an anaerobic thermophilic pure strain, *Carboxydothermus hydrogenoformans*. Specific hydrogen production rates and yields were investigated at initial biomass densities varying from 5 to 20 mg volatile suspended solid (VSS) L^{-1}. Results showed that the gas–liquid mass transfer limits the CO conversion rate at high biomass concentrations. At 100-rpm agitation and at CO partial pressure of 1 atm, the optimal substrate/biomass ratio must exceed 5 mol CO g^{-1} biomass VSS in order to avoid gas–liquid substrate transfer limitation. An average H_2 yield of 94±3% and a specific hydrogen production rate of ca. 3 mol g^{-1} VSS day^{-1} were obtained at initial biomass densities between 5 and 8 mg VSS^{-1}. In addition, CO bioconversion kinetics was assessed at CO partial pressure from 0.16 to 2 atm, corresponding to a dissolved CO concentration at 70°C from 0.09 to 1.1 mM. Specific bioactivity was maximal at 3.5 mol CO g^{-1} VSS day^{-1} for a dissolved CO concentration of 0.55 mM in the culture. This optimal concentration is higher than with most other hydrogenogenic carboxydotrophic species.

Y. Zhao · Z. Liu
Faculty of Chemical, Environmental and Biological Engineering,
Dalian University of Technology,
Dalian 116012, People's Republic of China

Y. Zhao · R. Cimpoia · S. R. Guiot (✉)
Biotechnology Research Institute,
National Research Council of Canada,
6100 Royalmount Avenue,
Montreal, QC, Canada H4P 2R2
e-mail: serge.guiot@cnrc-nrc.gc.ca

Keywords Syngas · Carbon monoxide · Hydrogen · *Carboxydothermus hydrogenoformans* · Kinetics · Inhibition · Gas–liquid mass transfer

Introduction

Sustainable hydrogen can be extracted from primary or secondary biomasses (industrial and municipal organic wastes, agriculture residues, biosolids, energy crops, algae) at a relatively elevated yield using a combination of hydrolytic, anaerobic fermentation and microbial electrosynthesis bioprocesses (Wang et al. 2011). However, a significant portion of biomass is difficult and/or slowly biodegradable by microorganisms due to its refractory and polymeric nature. When the organic residue is relatively dry (e.g., woodchips, beetle-infested wood, etc.) or non-biodegradable (bark, plastic, rubber, etc.), it might be more appropriate to use thermochemical conversion techniques such as gasification, which results in a synthesis gas (syngas) mainly composed of carbon monoxide (CO), carbon dioxide (CO_2), and hydrogen (H_2). Then syngas can be upgraded into H_2 using catalytic or biologically mediated water–gas shift (WGS) reaction to convert the carbon monoxide contained in syngas into hydrogen ($CO+H_2O \rightarrow CO_2+H_2$). An increasing number of carboxydotrophic microorganisms have been found to perform the biological WGS reaction, using CO as a preferred energy source (Wolfrum and Watt 2002). In brief, the oxidation of CO to CO_2 ($CO+H_2O \rightarrow CO_2+2H^++2e^-$) is catalyzed by a monofunctional Ni-containing CO dehydrogenase (CODH); electrons released are captured by an energy converting hydrogenase that reduces protons to molecular hydrogen; this is coupled to the membrane translocation of protons which can drive ATP synthesis. While this energy

conservation is thus independent of the acetyl-coenzyme A (CoA) pathway, the thermophilic, carboxydotrophic, hydrogenogenic microorganisms possess bifunctional acetyl-CoA synthase (ACS)/CODH complexes for carbon fixation. The acetyl-CoA is formed by binding a CoA, a CO, and a methyl group, the latter resulting from the reduction of CO_2 by reducing equivalents derived from the oxidation of CO (Uffen 1981; Bonam et al. 1989; Davidova et al. 1994; Svetlitchnyi et al. 2001; Lindahl 2002; Ragsdale 2004; Russell and Martin 2004; Henstra et al. 2007b; Oelgeschäger and Rother 2008; Sokolova et al. 2009). *Carboxydothermus hydrogenoformans*, one of those CO-oxidizing strains, is a strictly anaerobic, Gram-positive, extremely thermophilic bacterium that can grow in the dark on CO as the sole carbon and energy source (Gerhardt et al. 1991; Svetlichnyi et al. 1991, 1994; Henstra and Stams 2004). The cell culture density is limiting the CO conversion rate only when the cell concentration is low just after inoculation (Henstra 2006). However, because of the low aqueous solubility of CO, gas–liquid mass transfer turns out to be the limiting step of CO conversion once the growth of biomass has been sufficient, as the volumetric bioactivity potential of the *C. hydrogenoformans* culture becomes limited by the dissolved CO available in the liquid (Cowger et al. 1992; Kapic et al. 2006; Riggs and Heindel 2006; Jones 2007; Ungerman and Heindel 2007). Hence, for a thermophilic bioprocess to perform at a continuous maximal volumetric activity rate, it is essential for the cell concentration of the microorganism to be optimized to avoid the CO gas–liquid mass transfer limitation.

However, CO is both a substrate (electron donor and/or carbon source) and an inhibitor, and at elevated concentrations, can inhibit growth and catabolic activity due to its high affinity for metal-containing enzymes and hemes (Ragsdale 2004). The CO toxicity is not only the result of hydrogenase inhibition that may occur even at CO partial pressure (p_{CO}) as low as 0.05 atm (≈45 μM CO in solution, Soboh et al. 2002); CO inhibits also the acetyl-CoA synthesis, usually at higher concentrations. But typically a residual activity remains at the highest CO concentrations employed (Maynard et al. 2001; Amos 2004). Complete inhibition of direct conversion of CO into CH_4 and CO_2 by *Methanobacterium thermoautotrophicum* occurred at a p_{CO} of 0.6 atm (Daniels et al. 1977), whereas *Methanosarcina barkeri* could be slowly adapted to growth at 100% CO (O'Brien et al. 1984). Hurst and Lewis (2010) assessed the effects of CO (p_{CO} ranging from 0.35 to 2.0 atm) on cell growth, acetic acid, and ethanol production using *Clostridium carboxidivorans* $P7^T$. They found inter alia that the conversion of CO to acetic acid decreased beyond a p_{CO} of 0.7 atm. The maximal WGS activity of *Rubrivivax gelatinosus* CBS occurred at a dissolved CO concentration of 90–100 μM. Concentrations greater than 150 μM resulted in decreased reaction rate and eventual shutdown of the biological WGS pathway (Amos 2004). With *Archaeoglobus fulgidus*, CO levels up to 0.4 atm did not affect the culture activity, with or without co-substrate (lactate), while CO levels from 0.4 to 0.8 atm resulted in a noticeable decrease, which was more marked in the absence of lactate (Henstra et al. 2007a). X-ray crystallographic studies have shown that CO binds to the nickel ion at the active site of the [NiFe] hydrogenase from *Desulfovibrio vulgaris* Miyazaki F and inhibits its catalytic function (Pandelia et al. 2010). The CODH enzyme complex purified from *C. hydrogenoformans* showed maximal CO-oxidizing:H_2-evolving activity with 5% CO in the headspace, whereas higher CO concentrations inhibited the energy converting [NiFe] hydrogenase present in the enzyme complex (Soboh et al. 2002).

However, to our knowledge, the kinetics of the CO reaction by intact cells of the *C. hydrogenoformans* strain as a function of the CO partial pressure has never been reported in the literature. At the same time, improvement in the gas–liquid mass transfer may exacerbate the inhibition by increasing the availability of dissolved CO. To address those issues, the impact of the initial cell density as well as the initial CO partial pressure on the specific CO consumption and hydrogen production rates and biomass specific growth rate was investigated using *C. hydrogenoformans* pure cultures.

Material and methods

Culture

C. hydrogenoformans DSM6008 was obtained from the German Collection of Microorganisms and Cell Cultures, DSMZ (Deutsche Sammlung von Mikroorganismen und Zellkulturen GmbH). The strain was cultivated in shake culture at 100 rpm under strictly anaerobic conditions at 70°C in a basal mineral medium buffered with bicarbonate–phosphate. The medium was made in two steps. A solution containing (in milligrams per liter of demineralized water KCl 330, $MgCl_2{\cdot}6H_2O$ 102, $CaCl_2{\cdot}2H_2O$ 15, NH_4Cl 330, KH_2PO_4 136) was autoclaved, and then completed with (in milliliters per liter of solution) 5% $NaHCO_3$ stock solution (8), 2.5% $Na_2S{\cdot}9H_2O$ stock solution (10), 0.5% yeast extract solution (10), trace metals solution (10), and vitamin solution (1). The trace metals and vitamin stock solutions were prepared as described by Stams et al. (1993). All stock solutions were autoclaved, except the vitamin solution, which was sterilized by filtration through 0.22-μm filter membranes. The initial pH was adjusted between 6.8 and 7.0.

Growth and activity assays

The growth and activity tests were performed in triplicate in 60-mL serum glass bottles. Briefly, once inoculated with the centrifugation pellet of a given volume of culture and filled with the bicarbonate–phosphate-buffered mineral medium for a final volume of 30 mL, bottles were capped, sealed, and flushed with CO as sole carbon source and placed in a rotary shaker (New Brunswick, Edison, NJ, USA) in a dark, thermostatically controlled environment (70±1°C) and gyrated at 100 rpm. The growth tests were carried out under 1 atm of 100% CO. As reported previously (Svetlichnyi et al. 1991; Henstra and Stams 2004; Henstra 2006), the growth curve of the *C. hydrogenoformans* culture systematically exhibited a lag phase in the presence of CO that consists of two parts: one in which no CO is consumed, and one in which CO is consumed without cell multiplication. Consequently, the initial biomass concentration was measured 1 h after the bottle headspace was replenished with fresh 100% CO after the first CO phase, this being considered as time zero. Growth was estimated by difference between the biomass concentration values measured at this time zero and at the end of the test. Biomass concentration was quantified by optical density (OD) at 600 nm (Beckman DU-640 Spectrophotometer, Corona CA, USA). The OD data were subsequently converted to volatile suspended solid (VSS) biomass using a conversion factor previously determined as follows. The biomass concentration of *C. hydrogenoformans* culture dilutions ranging between 0.001 and 0.025 unit OD was assessed using chemical oxygen demand (COD) measurements which were then converted to VSS using a factor of 1.37 g COD g^{-1} VSS based on the elemental formula of microbial biomass as $CH_{1.79}O_{0.5}N_{0.2}S_{0.005}$ (Roels 1983). The correlation of the VSS data to their corresponding OD values (n=14; R^2=0.80) yielded a conversion factor of 1,666 mg VSS per unit OD.

For kinetics tests, each of a series of 60-mL serum bottles received 30 mL of culture suspension containing approximately 3.5 mg VSS L^{-1}. The headspace (30 mL) of all bottles was filled with different mixtures of CO and argon at a total pressure of 2 atm. The gas mixtures consisted of CO at initial p_{CO} ranging between 0 and 2 atm, the balance consisting of argon. Both substrate (CO) depletion and catabolite (H_2, volatile fatty acids, and alcohols) production were monitored. The specific CO uptake or H_2 production rates, expressed as mole CO g^{-1} VSS day^{-1} or mole H_2 g^{-1} VSS day^{-1}, respectively, were obtained by reporting the rate of CO consumed or H_2 produced (mole per day) to the VSS-based biomass as estimated in the bottle. The hydrogen yield (Y_{H_2}) was expressed as a percentage of the H_2 gas produced per CO consumed (mole per mole).

Analytical methods

The suspended solids, VSS, and COD were determined according to standard methods (Eaton et al. 2005). Volatile fatty acids (i.e., acetic, propionic, and butyric acids) were measured on an Agilent 6890 gas chromatograph (Wilmington, DE, USA) equipped with a flame ionization detector on 0.2-μL samples diluted 1:1 (vol./vol.) with an internal standard of isobutyric acid in 6% formic acid, directly injected on a glass column of 1 m×2 mm Carbopack C (60–80 mesh) coated with 0.3% Carbowax 20 M and 0.1% H_3PO_4. The column was held at 130°C for 4 min. Helium was the carrier gas fed at a rate of 20 mL min^{-1}. The injector and the detector were both maintained at 200°C. For the measurement of solvents (methanol, ethanol, acetone, 2-propanol, *tert*-butanol, *n*-propanol, *sec*-butanol, *n*-butanol), 100 μL of liquid was transferred into a vial that had 20 mL of headspace and was closed with a crimped Teflon-coated septum. The vial was heated at 80°C for 2 min, and then 1,000 μL of headspace gas was injected on a DB-ACL2 capillary column of 30 m×530 mm×2 μm using a Combipal autosampler (CTC Analytics AG, Zwingen, Switzerland). The column was held at 40°C for 10 min. Helium was the carrier gas at a head pressure of 5 psi. The injector and the detector were maintained at 200°C and 250°C, respectively. The gas composition (H_2, CO, CO_2) was measured by injecting 300 μL of gas (model 1,750 gas-tight syringe, Hamilton, Reno, NV, USA) taken from the bottle headspace after equilibrium at 70°C into a HP 6890 gas chromatograph (Hewlett Packard, Palo Alto, CA, USA) equipped with a thermal conductive detector and a 11-m×3.2-mm 60/80 mesh Chromosorb 102 packed column (Supelco, Bellafonte, PA, USA). The column temperature was held at 60°C for 7 min and increased to 225 C at a rate of 60°C/min. Argon was used as the carrier gas. The injector and detector were maintained at 125°C and 150°C, respectively.

Results

Impact of microbial density on H_2 yield and cell growth

Without mass transfer limitation, the observed rate of a biochemical reaction should be close to the maximal intrinsic reaction rate. In contrast, as CO is sparingly soluble, especially at 70°C, gas–liquid mass transfer rate can easily be limiting, depending on the pressure and

mixing conditions. Hence, for given mixing and pressure conditions, i.e., for a fixed mass transfer rate, volumetric bioactivity potential rate must be less than the gas–liquid mass transfer rate for the latter not to curb the bioactivity kinetics. In principle, volumetric bioactivity rate increases proportionally to the microbial density. In other words, there is a biomass density level below which the volumetric bioactivity would be kinetics-driven rather than transport-limited. To determine at which biomass density level the bioactivity rate is greater than the mass transfer rate, a series of tests were conducted at microbial concentrations (X_o) varying between ca. 5 and 25 mg VSS L^{-1}, while keeping constant CO pressure (1 atm) and agitation rate (100 rpm). Specific rates of CO uptake, biomass specific growth, and specific hydrogen production rates were investigated as a function of the biomass densities.

The specific hydrogen production rate results were plotted as a function of the initial biomass density shown in Fig. 1. The graph shows clearly a twofold greater specific activity rate at the lowest cell density range, at a level of ca. 3 mol H_2 g^{-1} VSS day^{-1} as opposed to 1.5–1.7 mol H_2 g^{-1} VSS day^{-1} at higher cell density. These production rate levels corresponded to CO uptake values of the same order, i.e., 2.8±0.6 and 1.5±0.2 mol CO g^{-1} VSS day^{-1}, respectively, as expected since the yield of CO conversion into H_2 is theoretically 1 mol mol^{-1}. So this readily leads us to conclude that biomass density above an 8–9-mg VSS L^{-1} range resulted in a volumetric activity rate above the mass transfer rate for the test conditions fixed at 100 rpm agitation at 1 atm CO partial pressure. In other words, the volumetric rate observed for those biomass densities above 8–9 mg VSS L^{-1} must be read as the volumetric gas–liquid mass transfer rate, constant and equivalent to 45±7 mmol CO L^{-1} day^{-1}, for those set conditions. It is concluded as well that *C. hydrogenoformans* has an intrinsic biological WGS reaction rate, normally close to its maximal specific activity potential, at ca. 3 mol H_2 or CO g^{-1} VSS day^{-1}. Similar trends were also observed with the growth as a function of the cell density. The empirical biomass growth rate (μ_o) was assessed by the difference between the VSS content values in the bottles at the beginning and the end of the tests ($\Delta X = X_f - X_o$), reported for the time span (Δt), and the median biomass content ($X_o + \Delta X/2$). In first approximation, the growth-specific rates could be grouped at two levels: with the highest values (1.03±0.28 day^{-1}) at the low cell density range and the lowest values (0.55±0.30 day^{-1}) above a microbial concentration of 9 mg VSS L^{-1}.

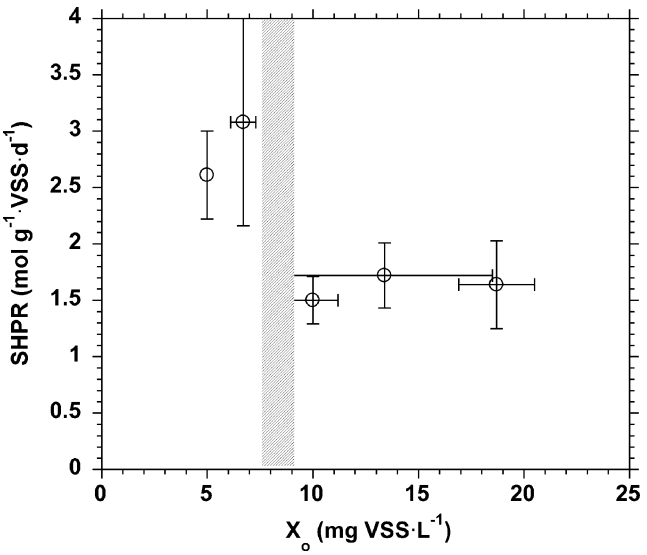

Fig. 1 Effect of initial microbial density (X_o) on the specific hydrogen production rate (*SHPR*) of *C. hydrogenoformans*

There was no significant difference between the hydrogen and growth yields at any biomass concentration. The H_2 yield fluctuated between 83% and 98% (mole per mole), which corresponded to an average yield of 93±4%. Other co-products were also detected (essentially acetate and ethanol), but in trace amounts and always less than 3% of the substrate uptake. On one hand, the growth yield (Y_G) can be estimated by mass balance from the H_2 yield. According to the acetyl-CoA pathway involved in the carbon fixation for the culture to grow, half of the CO not consumed for H_2 production is assimilated. For two carbons to be fixed during biomass synthesis, the microbe uses one CO and one CO_2 to build one acetyl-CoA from HSCoA plus three additional CO to produce the three pairs of reducing equivalents (2[H]) to reduce the assimilated CO_2 into a methyl group (Fig. 2). This means that the true growth yield relates to half the balance between the number of CO moles consumed and the number of H_2 moles produced. The true growth yield values obtained from the balance between the CO consumed and the H_2 produced (with 12-g biomass C mol^{-1} CO assimilated and 0.47 g C g^{-1} biomass VSS, Roels 1983) fluctuated between 0.29 and 1.22 g VSS mol^{-1} CO, which corresponds to an average growth yield of 0.68±0.26 g VSS mol^{-1} CO. On the other hand, the observed biomass change (ΔX) corresponding to the CO consumed gave growth yields fluctuating between 0.26 and 0.91 g VSS mol^{-1} CO, which corresponded to an average growth yield of 0.46±0.20 g VSS mol^{-1} CO. Besides the experimental error, there is one reason to explain the discrepancy between the two approaches. The latter yield is based on the observed growth (i.e., true growth minus biomass decay, i.e., cell death and endogenous catabolism), while the former yield does not account for biomass decay.

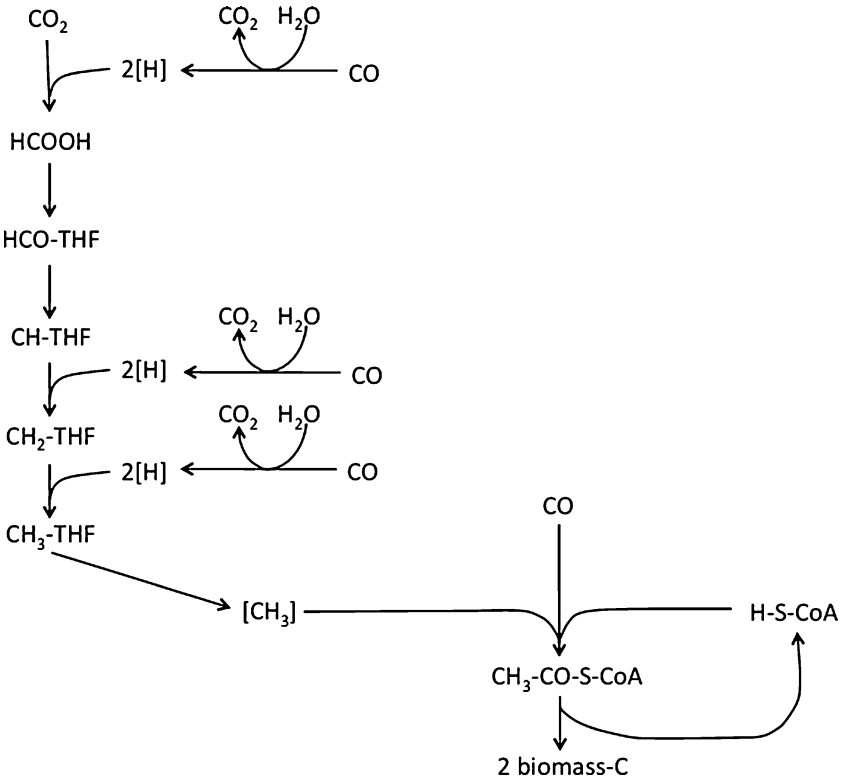

Fig. 2 Schematic representation of the reductive acetyl-CoA pathway involved in the carbon fixation for biomass synthesis. Oxidation of CO with H_2O to CO_2 and 2[H] provides reducing equivalents for the reduction of CO_2 to formate (HCOOH), of methylenetetrahydrofolate (CH–THF) to methenyltetrahydrofolate (CH_2–THF), and of CH_2–THF to methyltetrahydrofolate (CH_3–THF). ACS/CODH catalyzes the formation of acetyl-CoA from a bound methyl group, CO and coenzyme A (*CoA*) (Henstra et al. 2007b)

CO conversion kinetics and inhibition

To determine CO concentration optima, CO uptake activity tests were performed under different initial p_{CO} varying from 0.16 to 1.94 atm. Those p_{CO} values corresponded to dissolved CO concentrations from 0.09 to 1.10 mM, using a value of 1,766 atm Lmol^{-1} for the Henry constant at 70°C (Lide 1999). Subsequent to the findings reported in the previous section, the culture was diluted in anaerobic phosphate buffer at an initial biomass density of 3.5 mg VSS L^{-1} in order to avoid gas–liquid mass transfer limitation, hence to make sure that measured rates are kinetics-driven. The results are displayed in Fig. 3. Specific activity increased with increasing dissolved CO concentration up to a maximum of 3.3–3.5 mol CO g^{-1} VSS day^{-1} at a CO level of 0.55 mmol L^{-1} (i.e., ~ca. 1 atm). Beyond that optimal CO, the activity decreased sharply down to values as low as 0.5 mol CO g^{-1} VSS day^{-1} (i.e., 15% of the maximum activity rate).

The Han and Levenspiel (1988) model used to fit kinetics curve through the data points is described by Eq. 1, where k and k_{max} are the measured and maximal specific rates of substrate (S) depletion, respectively, dissolved CO being the substrate in this case; K_M is the half-saturation constant (the Michaelis constant); S_I is the critical concentration of the inhibitory substrate above which reaction stops; n and m are empirical constants. Equation 1 can be simplified as shown in Eq. 2 at high substrate concentration [$S \gg K_M(1 - S/S_I)^m$] when inhibition occurs.

$$k = k_{max}\left(1 - \frac{S}{S_I}\right)^n \frac{S}{S + K_M(1 - S/S_I)^m} \quad (1)$$

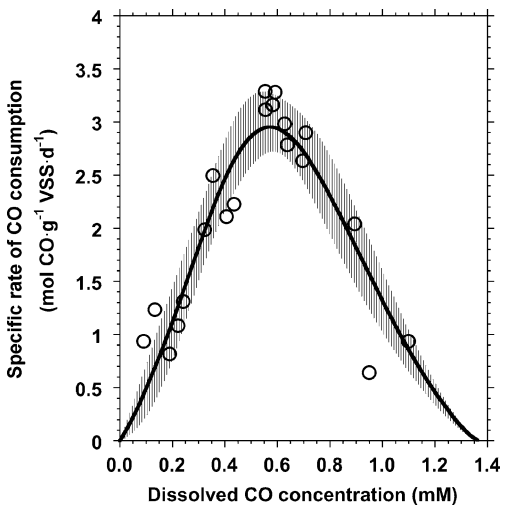

Fig. 3 Kinetics of CO consumption-specific activity of *C. hydrogenoformans* as a function of the dissolved CO concentration. Experimental data (*white circle*) and Eq. 1 fit curve (*line*) with k_{max}=8.2 mol CO g^{-1} VSS day^{-1}, K_M=2.1 mM, S_I=1.37 mM, n=1.4, and m=4.7. *Hatching*: 95% confidence band

$$k = k_{\max}\left(1 - \frac{S}{S_I}\right)^n \quad (2)$$

For the constants estimation, we followed the two-step procedure outlined by Han and Levenspiel, except that we used nonlinear regression to fit the data to the equations. The curve fit was based on the Levenberg–Marquardt algorithm and calculated using an iterative procedure to find the best fit with the lowest sum of the squared errors between the original data and the calculated fit (Prism v. 4.0, GraphPad Software Inc., San Diego, CA, USA). First, nonlinear regression was applied to fit Eq. 2 to the data range corresponding to the highest substrate concentrations (from 0.58 to 1.1 mM), to estimate k_{max}, S_I, and n. We found k_{max}=7 mol CO g^{-1} VSS day^{-1}, S_I=1.37 mM, and n=1.4, with a coefficient of determination (R^2) of 0.88. However, the 95% confidence interval (CI_{95}) for k_{max} was relatively large, from −0.4 to 14.5. Therefore, we used the second step to both refine the k_{max} estimate and assess the value of other constants, K_M and m. To do so, nonlinear regression was applied to the entire range of data to fit Eq. 1 with the S_I and n constants constrained to the values found above, i.e., 1.37 mM and 1.4, respectively. We found k_{max}=8.2 mol CO g^{-1} VSS day^{-1} (CI_{95}, 6.3 to 10.1), K_M=2.1 mM (CI_{95}, 0.8 to 3.4), and m=4.7 (CI_{95}, 1.8 to 7.6). The similarity between the two k_{max} values found separately is indicative of the correctness of this stepwise approach. The best fit curve is plotted along with the experimental data points shown in Fig. 3; the absolute sum of squared errors between the calculated and experimental data equals 2.3 and R^2, 0.86. The fit seems reasonable with most of the experimental data points falling inside the 95% confidence band (Fig. 3).

Discussion

The yield values for both H_2 and growth assessed in this study are generally consistent with literature data specific for *C. hydrogenoformans* (Table 1). The Han and Levenspiel model is well suited to such typical substrate inhibition kinetics, as reviewed previously (Fountoulakis et al. 2008). As expected, the value found for k_{max} was high (8.2 mol CO g^{-1} VSS day^{-1}), as compared to the one observed in this study (3.5 mol CO g^{-1} VSS day^{-1}) or the ones reported in the literature (Table 1, 0.6–3.9 mol CO g^{-1} VSS day^{-1}). This reflects that the kinetic activity potential of the strain could be high if CO were not at all an inhibitor, but only an activator. This is confirmed by the k_{max} and K_M values (10.6 mol CO g^{-1} VSS day^{-1} and 1.45 mM, respectively) found by fitting the Monod model [$k = k_{max}S/(K_M + S)$] to the data range corresponding to CO concentrations lower than 0.55 mM (R^2=0.89). According to Han and Levenspiel, the relative magnitude of the constants m and n relates to the inhibition pattern. When both m and n constants are greater than zero, this represents generalized uncompetitive inhibition. This is consistent with the conclusion of Maynard et al. (2001) that the CO inhibition of ACS purified from *Clostridium thermoaceticum* was uncompetitive.

The kinetics of *C. hydrogenoformans* compares favorably with those of other bacteria able to perform the WGS reaction. The maximal WGS activity of *R. gelatinosus* CBS occurred at a dissolved CO concentration of ca. 0.1 mM (Amos 2004). Whole cells of *Proteus vulgaris* started to be inhibited at a CO concentration of 0.055 mM, while hydrogenases purified from *Desulfovibrio desulfuricans* began to be inhibited at an even lower concentration of 0.003 M (Purec et al. 1962). The intact cells may offer more resistance to CO toxicity than their purified enzymes. Indeed, a CODH enzyme complex purified from *C. hydrogenoformans* showed maximal CO-oxidizing:H_2-evolving activity at a CO level in the headspace as low as 5% (0.03 mM at 70°C) as well (Soboh et al. 2002). However, the analysis of the genome of *C. hydrogenoformans* revealed the remarkable presence of at least five highly differentiated CODH complexes (Wu et al. 2005). This likely explains in part why this species was able to grow more rapidly on CO and to exhibit more resistance to the CO toxicity than other hydrogenogenic carboxydotrophic species.

Table 1 Yield and kinetics data of *C.*: comparison with literature

X_o, mg VSS L^{-1}	Specific activity, mol CO g^{-1} VSS day^{-1}	Y_{H_2} (%) (mol/mol)	Y_G, g (d. wt) mol^{-1} CO	Reference
135–277	1.2–0.6	98.9	0.57–1.17[a]	Svetlichnyi et al. (1991)
197	3.9	82.3	1.18[b]	Henstra (2006)
15–30	3.6–1.7	72.7–80	0.52–1.06[a]	Gerhardt et al. (1991)
3.5	3.5	83–98	0.29–1.22	This study

[a] Data range, based on either 4.89 10^{-13} (Loferer-Krössbacher et al. 1998) or 10^{-12} g (d. wt)/cell (Davis et al. 1973)

[b] Calculated with data from graphs

Acknowledgments The authors thank C. Peter, M-J Lévesque, and M. Haddad for their assistance and discussions. One of the authors (YZ) was supported by the Canada NRC-China MOE Research and Postdoctoral Fellowship Program. This is NRCC paper no. 53371.

References

Amos WA (2004) Biological water–gas shift conversion of carbon monoxide to hydrogen. Milestone Completion Report for the US Department of Energy, HFCIT Program. Report no.: NREL/MP-560-35592, National Renewable Energy Laboratory (NREL), Golden

Bonam D, Lehman L, Roberts GP, Ludden PW (1989) Regulation of carbon monoxide dehydrogenase and hydrogenase in *Rhodospirillum rubrum*: effects of CO and oxygen on synthesis and activity. J Bacteriol 171:3102–3107

Cowger JP, Klasson KT, Ackerson MD, Clausen E, Caddy JL (1992) Mass transfer and kinetic aspects in continuous bioreactors using *Rhodospirillum rubrum*. Appl Biochem Biotechnol 34/35 (1):613–624

Daniels L, Fuchs G, Thauer RK, Zeikus JG (1977) Carbon monoxide oxidation by methanogenic bacteria. J Bacteriol 132:118–126

Davidova MN, Tarasova NB, Mukhitova FK, Karpilova FK (1994) Carbon monoxide in metabolism of anaerobic bacteria. Can J Microbiol 40:417–425

Davis BD, Dulbecco R, Eisen HN, Ginsberg HS, Wood WB (1973) Microbiology, 2nd edn. Harper and Row, Hagerstown, pp 96–97

Eaton AD, Clesceri LS, Rice EW, Greenberg AE (eds) (2005) Standard methods for the examination of water and wastewater, 21st edn. American Public Health Association, American Water Works Association, Water Environment Federation, Washington

Fountoulakis MS, Stamatelatou K, Lyberatos G (2008) The effect of pharmaceuticals on the kinetics of methanogenesis and acetogenesis. Bioresour Technol 99(15):7083–7090

Gerhardt M, Svetlichny V, Sokolova TG, Zavarzin GA, Ringpfeil M (1991) Bacterial CO utilization with H_2 production by strictly anaerobic lithoantotrophic thermophilic bacterium *Carboxydothermus hydrogenus* DSM6008 isolated from a hot swamp. FEMS Microbiol Lett 83(3):267–272

Han K, Levenspiel O (1988) Extended Monod kinetics for substrate, product and cell inhibition. Biotechnol Bioeng 32:430–437

Henstra AM (2006) CO metabolism of *Carboxydothermus hydrogenoformans* and *Archaeoglobus* fulgidus. Ph.D. Thesis, Wageningen University, Wageningen

Henstra AM, Stams AJM (2004) Novel physiological features of *Carboxydothermus hydrogenoformans* and *Thermoterrabacterium ferrireducens*. Appl Environ Microbiol 70(12):7236–7240

Henstra AM, Dijkema C, Stams AJM (2007a) *Archaeoglobus fulgidus* couples CO oxidation to sulfate reduction and acetogenesis with transient formate accumulation. Environ Microbiol 9(7):1836–1841

Henstra AM, Sipma J, Rinzema A, Stams AJM (2007b) Microbiology of synthesis gas fermentation for biofuel production. Curr Opin Biotechnol 18(3):200–206

Hurst KM, Lewis RS (2010) Carbon monoxide partial pressure effects on the metabolic process of syngas fermentation. Biochem Eng J 48(2):159–165

Jones ST (2007) Gas liquid mass transfer in an external airlift loop reactor for syngas fermentation. Ph.D. Thesis. Iowa State University, Ames

Kapic A, Jones ST, Heindel TJ (2006) Carbon monoxide mass transfer in a syngas mixture. Ind Eng Chem Res 45(26):9150–9155

Lide DR (ed) (1999) CRC handbook of chemistry and physics, 80th edn. CRC, Boca Raton

Lindahl PA (2002) The Ni-containing carbon monoxide dehydrogenase family: light at the end of the tunnel? Biochemistry 41 (7):2097–2105

Loferer-Krössbacher M, Klima J, Psenner R (1998) Determination of bacterial cell dry mass by transmission electron microscopy and densitometric image analysis. Appl Environ Microbiol 64(2):688–694

Maynard EL, Sewell C, Lindahl PA (2001) Kinetic mechanism of acetyl-CoA synthase: steady-state synthesis at variable CO/CO_2 pressures. J Am Chem Soc 123(20):4697–4703

O'Brien JM, Wolkin RH, Moench TT, Morgan JB, Zeikus JG (1984) Association of hydrogen metabolism with unitrophic or mixotrophic growth of *Methanosarcina barkeri* on carbon monoxide. J Bacteriol 158(1):373–375

Oelgeschäger E, Rother M (2008) Carbon monoxide-dependent energy metabolism in anaerobic bacteria and archea. Arch Microbiol 190(3):257–269

Pandelia ME, Ogata H, Currell LJ, Flores M, Lubitz W (2010) Inhibition of the [NiFe] hydrogenase from *Desulfovibrio vulgaris* Miyazaki F by carbon monoxide: an FTIR and EPR spectroscopic study. Biochim Biophys Acta 1797(2):304–313

Purec L, Krasna AI, Rittesberg D (1962) The inhibition of hydrogenase by carbon monoxide and the reversal of this inhibition by light. Biochemistry 1(2):270–275

Ragsdale SW (2004) Life with carbon monoxide. Crit Rev Biochem Mol Biol 39:165–195

Riggs SS, Heindel TJ (2006) Measuring carbon monoxide gas–liquid mass transfer in a stirred tank reactor for syngas fermentation. Biotechnol Prog 22(3):903–906

Roels JA (1983) Energetics and kinetics in biotechnology. Elsevier Biomedical, Amsterdam

Russell MJ, Martin W (2004) The rocky roots of the acetyl-CoA pathway. Trends Biochem Sci 29(7):358–363

Soboh B, Linder D, Hedderich R (2002) Purification and catalytic properties of a CO-oxidizing:H2-evolving enzyme complex from *Carboxydothermus hydrogenoformans*. Eur J Biochem 269 (22):5712–5721

Sokolova TG, Henstra A-M, Sipma J, Parshina SN, Stams AJM, Lebedinsky AV (2009) Diversity and ecophysiological features of thermophilic carboxydotrophic anaerobes. FEMS Microbiol Ecol 68(2):131–141

Stams AJM, Van Dijk JB, Dijkema C, Plugge CM (1993) Growth of syntrophic propionate-oxidizing bacteria with fumarate in the absence of methanogenic bacteria. Appl Environ Microbiol 59 (4):1114–1119

Svetlichnyi VA, Sokolova TG, Gerhardt M, Ringpfeil M, Kostrikina NA, Zavarzin GA (1991) *Carboxydothermus hydrogenoformans* gen. nov., sp. nov., a CO-utilizing thermophilic anaerobic bacterium from hydrothermal environments of Kunashir Island. Syst Appl Microbiol 14(3):254–260

Svetlichnyi VA, Sokolova TG, Kostrikina NA, Lysenko AM (1994) A new thermophilic anaerobic carboxydotrophic bacterium *Carboxydothermus restrictus* sp. nov. Microbiology 63(3):294–297

Svetlitchnyi V, Peschel C, Acker G, Meyer O (2001) Two membrane-associated NiFeS-carbon monoxide dehydrogenases from the anaerobic carbon-monoxide-utilizing eubacterium *Carboxydothermus hydrogenoformans*. J Bacteriol 183(17):5134–5144

Uffen RL (1981) Metabolism of carbon monoxide. Enzyme Microbial Technol 3:197–206

Ungerman AJ, Heindel TJ (2007) Carbon monoxide mass transfer for syngas fermentation in a stirred tank reactor with dual impeller configurations. Biotechnol Progr 23(3):613–620

Wang A, Sun S, Cao G, Wang H, Ren N, Wu W-M, Logan BE (2011) Integrated hydrogen production process from cellulose by combining dark fermentation, microbial fuel cells, and a microbial electrolysis cell. Bioresour Technol 102(5):4137–4143

Wolfrum EJ, Watt AS (2002) Bioreactor design studies for a hydrogen-producing bacterium. Appl Biochem Biotechnol 98(100):611–625

Wu M, Ren Q, Durkin AS, Daugherty SC, Brinkac LM, Dodson RJ, Madupu R, Sullivan SA, Kolonay JF, Nelson WC, Tallon LJ, Jones KM, Ulrich LE, Gonzalez JM, Zhulin IB, Robb FT, Eise JA (2005) Life in hot carbon monoxide: the complete genome sequence of *Carboxydothermus hydrogenoformans* Z-2901. PLoS Genet 1(5):e65